

Properties of Abaca/Epoxy Composites Modified by Activated Carbon Particles for Orthosis Application

Harini Sosiati,^{a,*} Muhammad Kosasih,^a Ankas Pamasti,^a Rahmad K. Adi,^a Sinin Hamdan,^b and Yusril Yusuf^c

Abaca fiber (AF), epoxy (EP), and activated carbon particle (ACPs) incorporated composites have been previously studied to improve their mechanical properties. A study on integrating AF and ACPs to reinforce EP has not been done for comparison. The current study investigates the mechanical (tensile and flexural) and physical (water absorption) properties of AF/EP composites with 20 vol% AF modified by ACPs at 1% to 10% levels, and ACPs/EP composite with 20 vol% ACPs. Optical and scanning electron microscopy examined ACPs and the composite's fracture surface morphologies. X-ray diffraction was used to identify the ACPs' phase. The results showed that adding 5 vol% ACPs to AF/EP led to an optimum tensile strength of 42.50 MPa, which was slightly lower than AF/EP (43.00 MPa), and an optimum flexural strength of 62.10 MPa, which was slightly higher than AF/EP (60.50 MPa). Besides, adding 20% ACPs to EP resulted in a tensile strength of 31.93 MPa, higher than the previous result of ACPs/EP (26.34 MPa), also by adding 20% ACPs. Introducing ACPs to AF/EP could reduce water absorption in the composite by 6.52%. The measured flexural modulus of AF/EP added with 5 vol% ACPs was selected as the best material used in the simulation of ankle-foot orthosis (AFO) by Autodesk Inventor integrated with ANSYS Workbench 2019 R1. Applying a load of 27 N resulted in a von Misses stress of 54.018 MPa and a deformation of 44.675 mm.

DOI: 10.15376/biores.18.4.7510-7523

Keywords: Abaca fiber; Activated carbon particle; Epoxy; Hybrid composite; Mechanical and physical properties

Contact information: a: Department of Mechanical Engineering, Faculty of Engineering, Universitas Muhammadiyah Yogyakarta, Yogyakarta 55183, Indonesia; b: Department of Mechanical and Manufacturing Engineering, Faculty of Engineering, Universiti Malaysia Sarawak, Kota Samarahan, Sarawak 94300, Malaysia, c: Department of Physics, Faculty of Mathematics and Natural Sciences, Universitas Gadjah Mada, Yogyakarta 55281, Indonesia; *Corresponding author: hsosiati@ft.umy.ac.id

INTRODUCTION

Epoxy (EP) is a thermoset polymer with outstanding properties such as moisture, chemical, and corrosion resistance, and good adhesion with some additive materials (Cai *et al.* 2021; Karak 2021). However, for high-performance applications, EP needs excellent and suitable reinforcement materials in the form of fibers (synthetic or natural) and/or particles (organic or inorganic). EP resin-based composites are developed for various applications. Industrial applications in electronics and automotive require the fire retardancy of EP resins. Moreover, polymer composite materials are designed to replace metals for orthotic and prosthetic applications because of their light weight,

biocompatibility, durability, and corrosion resistance. An orthotic is a device utilized to support or improve the functionality of an abnormal body part. A prosthetic is a device that replaces a nonfunctional body part (Singhal *et al.* 2017; Shahar *et al.* 2019).

Epoxy (EP) reinforced with kenaf fiber has been reviewed as an orthotic material. EP is one of the thermoset polymers commonly used for orthotic devices (Shahar *et al.* 2019). Further, glass fiber/polypropylene composite (Singhal *et al.* 2017), carbon fiber/poly(lactic acid) (PLA) composite (Walbran *et al.* 2016; Abdalsadah *et al.* 2021; Raj *et al.* 2022), carbon fiber (Takhakh and Abbas 2018), and polypropylene (Mavroidis *et al.* 2011) are some orthotic materials that have been reported. In principle, the materials used for orthotic applications should be compatible with the human body. The orthotic fabrics should be strong, flexible, breathable, lightweight, and secure for walking.

The current study used abaca fiber (*Musa textilis*) and organic particles of activated carbon to strengthen EP resin to fabricate the hybrid composite for orthotic materials. Previous studies (Punnamurthy *et al.* 2014; Sinha *et al.* 2018) on the mechanical properties of abaca fiber (AF)/EP composites have reported that adding AF improved the impact strength (Punnamurthy *et al.* 2014) and tensile strength (Sinha *et al.* 2018) of the AF/EP composites. The optimum Charpy impact strength (7.68 mJ/mm²) was attained at 40% AF loading. However, AF/EP composite fabricated by hand lay-up technique resulted in the highest tensile strength of 29.87 MPa by triple-layered AF-EP with 7.9 wt% of AF loading. Additionally, the tensile strength (26.34 MPa) and tensile modulus (2.9 GPa) of activated carbon particles (ACPs)/EP composite increased with ACPs concentration, and the optimum was reached at 15 wt% ACPs (Hunain *et al.* 2021). Other AC coir fiber/EP composites showed optimum tensile stress of 13.42 MPa with 4 wt% AC fiber content and the highest Izod impact strength of 276 J by adding 10 wt% AC coir fiber (Salleh *et al.* 2013). The highest palm kernel AC/EP composite's modulus elasticity of ~9 GPa and ultimate tensile strength of ~21 MPa were achieved by the palm kernel AC: EP ratio of 30:70 (Mohmad *et al.* 2018). The composite resulted in the lowest water absorption of 3.3% at a similar condition.

According to earlier studies, AF and ACPs are compatible with EP resin and enhance mechanical properties. The addition of ACPs to EP decreased water absorption. However, the integration of AF and ACPs reinforced epoxy resin has not been studied, despite expectations to obtain better properties. This study explores the AF/ACPs/EP hybrid composite's tensile and flexural properties and water absorption for ankle-foot orthosis (AFO) applications by simulation.

The composites studied are non-hybrid and hybrid. The non-hybrid EP (80 vol%) composites were reinforced with AF and ACPs in 20 vol%, respectively, and EP hybrid composites were filled with mixed AF and ACPs. The establishment of 80 vol% of the EP matrix is intended to cover the fillers (AF and ACPs) evenly. The EP composite reinforced with AF (20 vol%) is compared to that with ACPs (20 vol%) to understand the filler's predominance in strengthening the EP matrix. For hybrid composites, ACPs were varied by 1, 2, 3, 5, and 10 (vol%). In this case, adding ACP concentrations was decided according to the following previous studies: Sosiati *et al.* (2023) conducted a study on composites made of sisal, microcrystalline cellulose (MCC), and polymethyl methacrylate (PMMA). They found that adding 1 vol% of MCC resulted in the optimum mechanical properties. Another study on the kenaf/silica microparticle/EP composites (Sosiati *et al.* 2022) with varying silica concentrations of 1, 2, 3, and 5 (vol%) reported optimum mechanical properties from adding 2 vol% silica. Also, a study of dental composites with nanoparticle fillers of TiO₂/ZnO (1, 2, 3, 4, and 5%) found that adding 4% filler resulted in the highest

mechanical properties (Shakir *et al.* 2019). Therefore, this study investigated the effects of adding ACPs. It was hypothesized that the addition of ACPs higher than 5% would reduce the mechanical properties. The properties of hybrid composites are compared to those of non-hybrid composites to select the best material to be utilized in AFO applications by simulation.

Studies on the composite material applications of AFO have been reported (Na Rungsri and Meesane 2012; Dequan Zou *et al.* 2014; Singhal *et al.* 2016; Takhakh and Abbas 2018; Abdalsadah *et al.* 2021; Raj *et al.* 2022). These studies mostly used synthetic fiber-reinforced polypropylene (PP) and polylactic acid (PLA) (Singhal *et al.* 2016; Takhakh and Abbas 2018; Abdalsadah *et al.* 2021; Raj *et al.* 2022). Only Na Rungsri and Meesane (2012) studied laminated composites of silk fiber/resin compared to carbon fiber/resin and glass fiber/resin for AFO materials. The tensile strength of composite filled with silk fiber (55.27 ± 1.87 MPa) was comparable with that of glass fiber (56.4 ± 2.9 MPa) and slightly lower than that with carbon fiber (58.53 ± 5.29 MPa). It has been suggested that silk fiber has a good chance of being used for AFO. Accordingly, the experimental data of the selected composite are compared to the orthotic materials from previous studies used in commercial devices. Generally, to maintain safety and stability, orthotic materials require good mechanical properties in terms of tensile, flexural, and compressive strengths.

EXPERIMENTAL

Materials

The Research Institute for Sweeteners and Fiber (Balittas), located in Indonesia, supplied the AF. In EP resin, Bisphenol A epichlorohydrin and polyaminoamide hardener were used in a 1:1 ratio as the resin and hardener, respectively, to strengthen the EP resin matrix used in the production of hybrid composites. The ACPs supplied by Merck Millipore (CAS 7440-44-0) were sieved to 400 mesh ($\sim 74 \mu\text{m}$).

Composite Fabrication

The AFs used were untreated (UT) and alkali-treated (AT), in which alkalization of AF is described elsewhere (Sosiati *et al.* 2023). Non-hybrid composites of UT-AF/EP and AT-AF/EP were fabricated by 80 vol% EP. The hybrid composites were also made using 80 vol% and 20 vol% of mixed AT-AF and ACPs, which varied from 0 to 20 vol%. In this case, ACPs were first mixed with EP using a mixer at 70 rpm for around 5 min, then mixed with short AF in the mold by the hand lay-up method (Fig. 1) and hot pressed at 100°C for 30 min. Figures 1 a, 1 b, and 1 c show weighing AF short fibers and arranging the fiber on the mold, mixing ACPs with EP, and pouring the mixture of ACPs and EP on the arranged AF, respectively. The composite specimens and their compositions are summarized in Table 1.

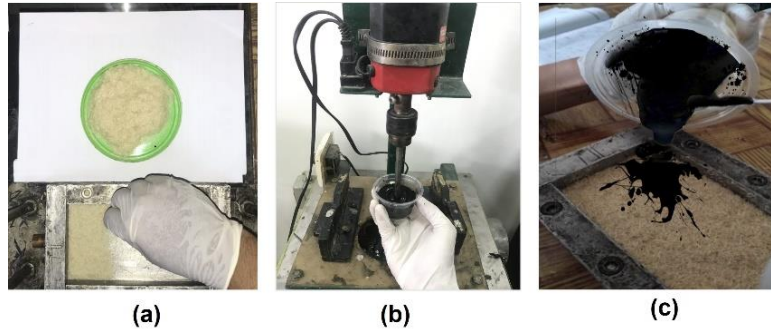


Fig. 1. Hand lay-up method of composite fabrication. (a) Weighing AF short fibers and arranging the fiber on the mold, (b) mixing ACPs with EP, and (c) pouring the mixture of ACPs and EP on the arranged AF

Table 1. Composite Specimens and Their Compositions

Specimen	Composition (vol%)		
	AF	ACPs	EP
UT-AF20/EP	20	-	80
AT-AF20/EP	20	-	80
AT-AF/ACPs ₁ /EP	19	1	80
AT-AF/ACPs ₂ /EP	18	2	80
AT-AF/ACPs ₃ /EP	17	3	80
AT-AF/ACPs ₅ /EP	15	5	80
AT-AF/ACPs ₁₀ /EP	10	10	80
ACPs ₂₀ /EP	-	20	80

UT: untreated, AT: alkali-treated, AF: abaca fiber, ACPs: activated carbon particles, and EP: epoxy

Mechanical and Physical Tests

All composite samples were tested by a three-point bending test with a maximum load of 20 kN and a crosshead speed of 2 mm/min on a universal testing machine (UTM, Zwick/Roell Z020). This test was completed in accordance with ASTM D790-03 (2003). The test specimen dimensions were $127 \times 12.7 \times 3.2$ mm³. The average of five measurements was then used to calculate the results. Using a similar machine, tensile tests on all composite specimens were conducted using the ASTM D638-14 (2014) standard with a maximum load of 20 kN and a crosshead speed of 10 mm/min. This study performed a simulation of AFO based on the measured flexural properties using Autodesk Inventor 2019 integrated with ANSYS Workbench 2019 R1 software (Ansys, Canonsburg, PA, USA). The load applied in this simulation was determined by a value that could reach the yield strength of the material used for AFO.

A water absorption test was also performed on all composite specimens following the ASTM D570-03 (2003) standard with a specimen size of $76.2 \times 25.4 \times 3.2$ mm. The test was performed for 336 h (2 weeks) by immersing the specimens in distilled water. The

specimens were weighed every 12 hours. The evaluation results are indicated by weight gain in percentage (%) according to the following Eq. 1,

$$M_i = (M_t - M_d)/M_d \times 100\% \quad (1)$$

where M_i is the percentage weight gain, M_t is the initial mass, and M_d is the mass at the interval measured.

RESULTS AND DISCUSSION

Activated Carbon Particles (ACPs) Phase and Morphology

Figures 2 (a) and 2 (b) show the SEM (JSM 6510A, Jeol Ltd., Tokyo, Japan) micrograph and XRD (Shimadzu XRD-7000; Shimadzu, Tokyo, Japan) profile of commercial ACPs. The ACPs used are micro-scale with uneven sizes. This is the ACP morphology after sieving with a 400-mesh sieve, and its surface morphology reveals the sub-micro pores, ranging from 200 to 300 nm, affected by the activation process (see a magnified image in Fig. 2a'). AC is commonly used as an adsorbent, which is related to the porosity on the AC surface. Activated carbon's hydrophobic/hydrophilic properties are correlated with its oxygen content, meaning that carbons containing a lot of oxygen show rather pronounced polarity, allowing water to be adsorbed preferentially (Ania *et al.* 2007). The effect of ACPs as the composite filler in this work is visible in the water absorption test results (Table 2).

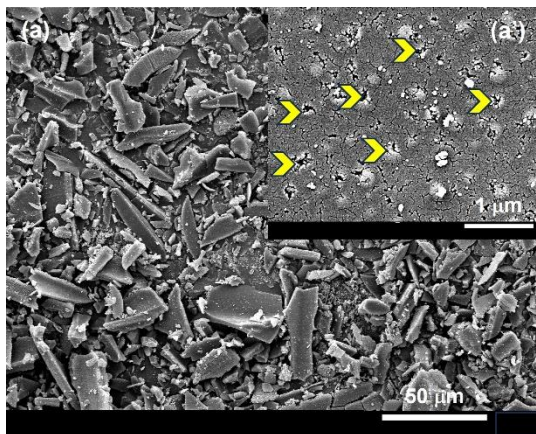


Fig. 2 (a). SEM images of ACPs, showing inhomogeneous particle size with sub-micro pores remarked by arrows in (a') decorated on the ACPs surface.

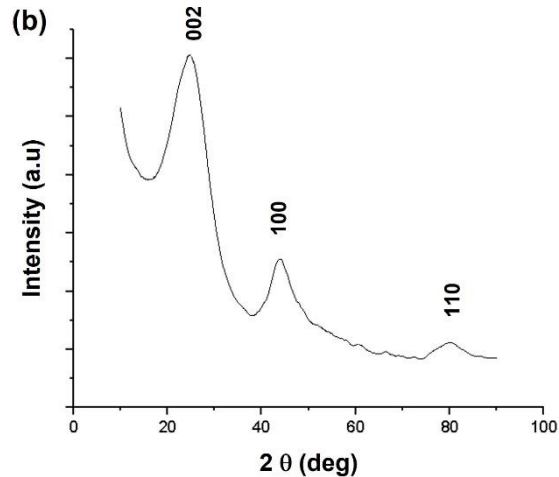


Fig. 2 (b). XRD profile of ACPs

The XRD peaks of 002, 100, and 110 crystalline planes were identified in ACPs but the intensity of a 110 peak is too low. The 002 peaks at $2\theta = 25.56^\circ$ indicate crystalline graphite. The 100 peak was unchanged before and after the carbon activation process (Lee *et al.* 2021). Therefore, the ACPs used in this work are present in crystalline and amorphous phases. It is considered that a broad peak of 100 contains an amorphous phase.

Tensile and Flexural Properties

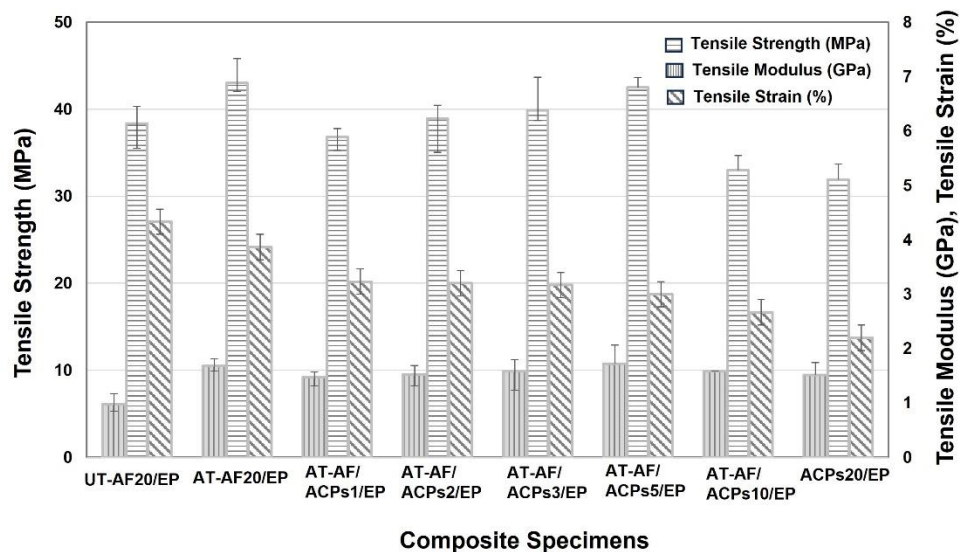


Fig. 3. Tensile properties of all composite specimens.

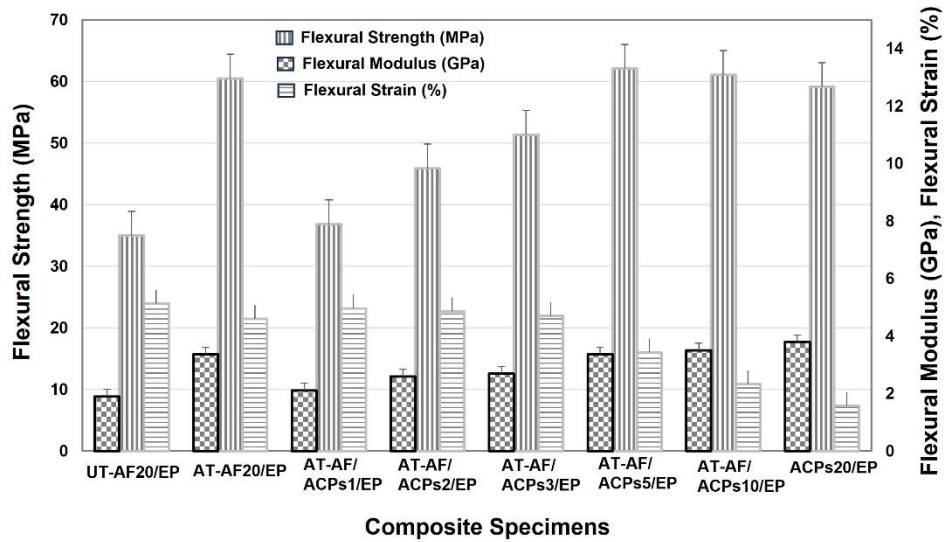


Fig. 4. Flexural properties of all composite specimens

Table 2. Tensile and Flexural Properties of Composite Specimens

Specimen	Tensile Properties			Flexural Properties		
	Tensile strength (MPa)	Tensile modulus (MPa)	Tensile strain (%)	Flexural strength (MPa)	Flexural modulus (MPa)	Flexural strain (%)
UT-AF20/EP	38.37±1.97	0.98±0.19	4.33±0.50	35.00±2.28	1.90±0.02	5.13±0.09
AT-AF20/EP	43.00±2.83	1.68±0.12	3.87±0.40	60.50±0.29	3.37±0.03	4.60±0.14
AT-AF/ACPs ₁ /EP	36.83±0.95	1.48±0.09	3.23±0.15	36.83±4.39	2.11±0.23	4.97±0.05
AT-AF/ACPs ₂ /EP	38.90±1.56	1.53±0.16	3.20±0.17	45.90±1.85	2.60±0.22	4.87±0.05
AT-AF/ACPs ₃ /EP	39.87±3.84	1.58±0.22	3.17±0.23	51.37±3.31	2.70±0.45	4.70±0.29
AT-AF/ACPs ₅ /EP	42.50±1.15	1.72±0.35	3.00±0.17	62.10±0.70	3.37±0.05	3.43±0.17
AT-AF/ACPs ₁₀ /EP	33.00±1.68	1.58±0.01	2.67±0.49	61.09±0.09	3.51±0.23	2.33±0.17
ACPs ₂₀ /EP	31.93±1.80	1.52±0.23	2.20±0.17	59.13±0.70	3.80±0.01	1.57±0.09

The tensile and flexural properties of all composite specimens (Table 1) are presented in Figs. 3 and 4. The property values are summarized in Table 2 to easily compare them among all composites. As is well known, alkalization improved the mechanical strengths (tensile and flexural); the properties of AT-AF20/EP were higher than those of UT-AF20/EP due to better interfacial adhesion between AF and EP surfaces. The addition of 1 vol% of ACPs reduced the mechanical strength, but a higher ACP concentration resulted in a higher mechanical strength, which achieved an optimum value by adding 5 vol% of ACPs (AT-AF/ACPs₅/EP). This result shows a similar trend in tensile and flexural strengths (Figs. 3 and 4). The addition of ACPs higher than 5 vol% leads to a decrease in mechanical strength. For the EP composite reinforced with only ACPs, the mechanical strain tends to be lower, indicating material embrittlement. Additionally, the changes in the modulus elasticities and mechanical strains caused by the addition of ACPs correspond to

the changes in the tensile fracture morphologies and cracks resulting from the bending test. These are discussed in the next paragraph.

Compared to the previous results, the tensile strength of AT-AF20/EP of 43 MPa was higher than that of AF/EP (29.87 MPa) (Sinha *et al.* 2018), despite differences in alkalization time. However, based on the authors' earlier study for kenaf/polypropylene (PP) composite, the tensile strength increased with alkalization time, and the maximum tensile strength reached around 47 MPa for a similar NaOH solution concentration for 36 h, whereas a minimum value showed 40 MPa for 4 h (Sosiati *et al.* 2019). Additionally, the tensile strength of the ACPs20/EP composite of 31.93 MPa was higher than that of AC/EP (26.34 MPa) with 15% AC loading (Hunain *et al.* 2021). The addition of AT-AF and ACPs to EP resulted in a significant increase in the tensile strength of EP (≤ 25 MPa) (Hunain *et al.* 2021). As shown in Figs. 2 and 3, when 5 vol% ACPs were added to the AT-AF/EP composite, it almost had the same mechanical strength and modulus (tensile and flexural) as the AT-AF/EP composite without ACPs. However, the addition of ACPs decreased the composite's strain.

Water Absorption

To understand the significant effect of adding ACPs on the composite's water absorption, the test was only conducted on five specimens (without and with ACPs), as summarized in Table 3. It is well known that the natural fiber composite has high water absorption, as shown in these results (Table 3), due to the AF's hydrophilicity. The presence of ACPs decreased water absorption because of their hydrophobicity, as discussed in the previous paragraph. However, the ACPs20/EP composite has the lowest strain, indicating its embrittlement.

Table 3. Water Absorption of the Composites Specimens

Specimen	Water Absorption (%)
UT-AF20/EP	22.91
AT-AF20/EP	15.50
AT-AF/ACP _s 5/EP	7.76
AT-AF/ACP _s 10/EP	6.52
ACP _s 20/EP	1.11

Microstructural Characterization

Figure 5 shows SEM (Zeiss Evo 10; Carl Zeiss Microscopy GmbH, Jena, Germany) images of the tensile fractured surface of all composite specimens. The composite specimens without ACPs (UT-AF20/EP and AT-AF20/EP) show no micro-voids, but open pores (blue arrows) formed in all composite specimens with ACPs. This is because water molecules were trapped when EP and ACPs were mixed, which was not done in a vacuum chamber. Especially in the AT-AF/ACP_s10/EP composite, open and closed pores (blue and white arrows, respectively) were observed, while adhesion between AF and EP surfaces was mostly good in all composites (red arrows), though debonding was also identified in some specimens (green arrows). These tensile fracture surface morphologies have a good relationship with the alteration of tensile properties (Fig. 3). Moreover, the surface morphology shown in the ACP_s20/EP composite (Fig. 5 h) indicates a brittle fracture

surface. Nevertheless, cracks were observed in the composite specimens with ACPs, making the composite's tensile properties lower than its flexural properties.

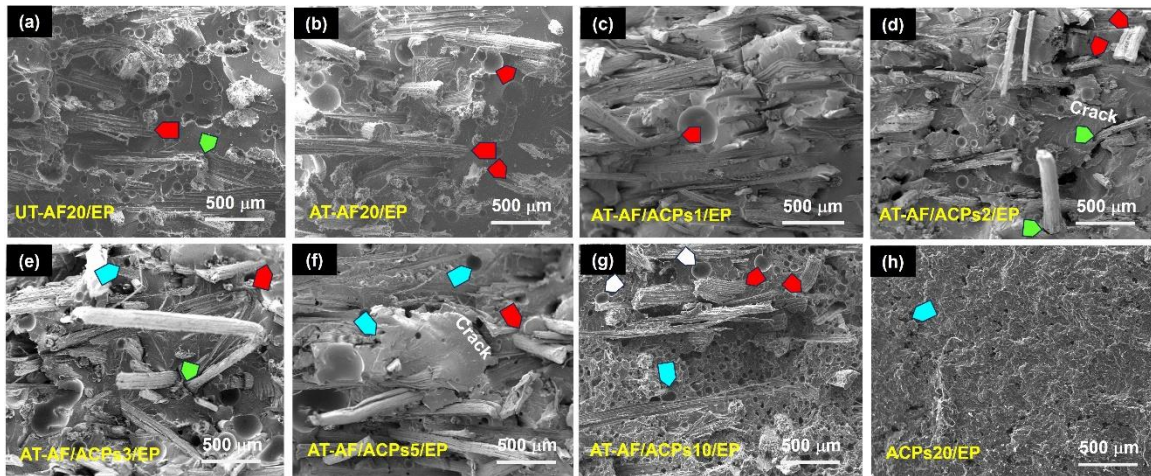


Fig. 5. SEM micrographs of tensile fracture surface for all composite specimens. Arrows show some characteristics formed on the fractured surfaces: *i.e.*, good bonding between AF and EP (red arrows), debonding (green arrows), open pores (blue arrows), and closed pores (white arrows).

Based on the results of observing how cracks formed in the composite specimens during the bending test, cracks were seen in the composites with ACPs as soon as 3 vol% to 20 vol% ACPs were added, as observed in optical micrographs Figs. 6e, 6f, 6g, and 6h. The composite specimen without AF was completely broken. That means 5 vol% ACPs is the maximum concentration that should be added to the AF/EP composite to achieve optimum tensile and flexural properties. These results were characterized with an optical microscope (Olympus SZ61; Olympus, Tokyo, Japan).

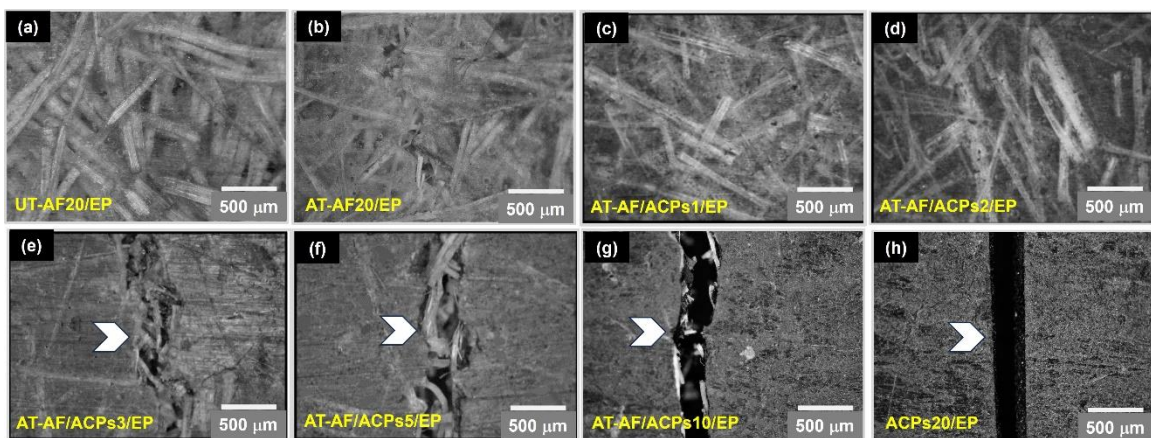


Fig. 6. Optical micrographs of the bending test of all composite specimens show cracks (marked with arrows) at the bottom sides.

Potential Application for AFO

Based on the mechanical properties and water absorption results discussed above, the AT-AF/ACPs5/EP composite was chosen for the AFO application. The AT-AF/ACPs5/EP composite's properties that resulted from this study are compared with the materials that have been investigated and commercially produced for AFO (Table 4). According to the comparison data in Table 4, the AT-AF/ACPs5/EP composite's tensile and flexural strengths are higher than those of PP, GF/PP, and CF2.5/PLA. In this application, PP seemed to be produced commercially. The AT-AF/ACPs5/EP composite's flexural modulus is higher than PP and CF2.5/PLA. The CF2.5/PLA composite has been studied by simulation and produced as a prototype.

Table 4. Comparison of Material Properties Used for AFO Applications

Material	Tensile Properties		Flexural Properties		References
	Tensile Strength (MPa)	Tensile Modulus (GPa)	Flexural Strength (MPa)	Flexural Modulus (GPa)	
AT-AF/ACPs5/EP	42.5	1.72	62.10	3.37	Present Study
Polypropylene (PP)	31	1.5	55	1.10	Mavroidis <i>et al.</i> 2011
Non-woven Glass fiber (GF)/PP	~29	2.25	-	-	Singhal <i>et al.</i> 2016
Carbon Fiber (CF)	105.7	2	-	-	Takhakh and Abbas, 2018
CF2.5/ polylactic acid (PLA)	37	3.2	60	3.1	Abdalsadah <i>et al.</i> 2021
C/PLA	-	3.9	-	-	Raj <i>et al.</i> 2022
Laminated Silk fiber/resin (3 layers)	55.27	-	-	-	Na Rungsri and Meesane, 2012

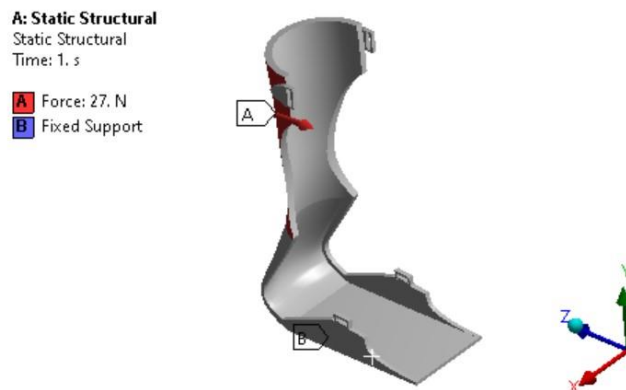


Fig. 7. The 3D model of AFO with an applied force of 27 N

In this study, the application AFO of the AT-AF/ACPs/EP composite was performed by simulation on the composite's flexural modulus. In this simulation, the force was progressively applied until it achieved the yield strength of the composite material of 55 MPa, where the maximum force load applied was 27 N. If a force load of more than 27 N is applied, the yield strength will be exceeded. The 3D model designed for AFO with an applied force of 27 N is shown in Fig. 7. In this study, the 3D model of AFO used a thickness of 3.5 mm. In the manufacturing guideline for AFO, the thicknesses usually used are 3 mm, 4 mm, or 5 mm depending upon the patient's weight (Orthosis 2006). Additionally, the 3D model of AFO for PP and high-density polyethylene (HDPE) was 3 mm and 4 mm, respectively (Kubasad *et al.* 2020). The AFO simulation resulted in a von Misses stress of 54.018 MPa (Fig. 8a) and a deformation of 44.675 mm (Fig. 8b).

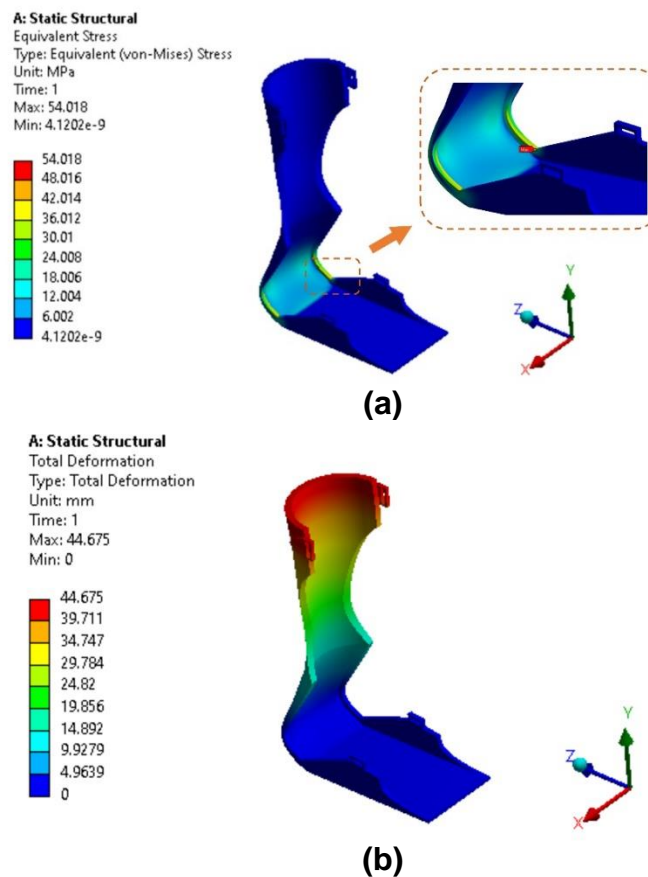


Fig. 8. The simulation results of a von Misses stress (a) and a deformation (b)

The earlier study (Raj *et al.* 2022) used a different simulation model from this study to run an AFO simulation based on the 3.9 MPa tensile modulus of the C/PLA composite. The applied load of 345.4 N yielded the deformation; the fracture distance from the sole was 49.67 mm. This deformation was slightly higher than what resulted in this study (44.67 mm). Because the simulation model was different, leading to a difference in the distribution of maximum deformation. However, the AT-FA/ACPs5/EP composite could be bent when it is applied for AFO. Therefore, this composite is considered to have the potential to be developed as an AFO material.

CONCLUSIONS

1. The role of alkali-treated abaca fiber (AT-AF) in strengthening epoxy (EP) composites is stronger than activated carbon particles (ACPs). Overall, the addition of ACPs to AT-AF/EP composites reduced tensile strength and strain, flexural strength and strain, and water absorption. However, among the AT-AF/ACPs/EP hybrid composites, adding 5 vol% ACPs resulted in the highest tensile and flexural strengths. Adding ACPs higher than 5% decreased the composite's mechanical properties.
2. There is no significant effect of ACPs on the composite's tensile modulus, but it led to crack formation soon after adding 3 vol% ACPs while decreasing the flexural strains. In the absence of AF in the composite (ACPs20/EP), the composite was completely broken. As a result, the hybrid composite of AT-AF/ACPs5/EP is selected for AFO material.
3. AFO simulation using the AT-AF/ACPs5/EP composite's flexural modulus yielded a von Misses stress of 54.018 MPa and a deformation of 44.675 mm, which showed almost the same as those of C/PLA AFO material: *i.e.*, 50.210 MPa and 49.67 mm, respectively. This finding pointed out that this composite could be a promising AFO material.

ACKNOWLEDGMENTS

The authors gratefully acknowledge the Ministry of Education, Culture, Research, and Technology, the Republic of Indonesia, for supporting this experimental research through the "*Penelitian Dasar Unggulan Perguruan Tinggi*" research grant under Contract No. 075/E5/PG.02.00.PL/2023.

REFERENCES CITED

- Abdalsadah, F. H., Hasan, F., Murtaza, Q., and Khan, A. A. (2021). "Design and manufacture of a custom ankle-foot orthoses using traditional manufacturing and fused deposition modeling," *Progress in Additive Manufacturing* 6(3), 555–570. DOI: 10.1007/s40964-021-00178-2
- Ania, C. O., Cabal, B., Parra, J. B., and Pis, J. J. (2007). "Importance of the hydrophobic character of activated carbons on the removal of naphthalene from the aqueous phase," *Adsorption Science and Technology* 25(3–4), 155–167. DOI: 10.1260/026361707782398164
- ASTM D570-03 (2003). "Water absorption 24 hour/equilibrium," ASTM International, West Conshohocken, PA, USA.
- ASTM D638-14 (2014). "Standard test method for tensile properties of plastics," ASTM International, West Conshohocken, PA, USA.
- ASTM D790-03 (2003). "Standard test methods for flexural properties of unreinforced and reinforced plastics and electrical insulating materials," ASTM International, West Conshohocken, PA, USA.

- Cai, W., Yuan, Z., Wang, Z., Guo, Z., Zhang, L., Wang, J., Liu, W., and Tang, T. (2021). "Enhancing the toughness of epoxy resin by using a novel hyperbranched benzoxazine," *Reactive and Functional Polymers* 164(March), Article ID 104920. DOI: 10.1016/j.reactfunctpolym.2021.104920
- Hunain, M. B., Alnomani, S. N., and Razzaq, Q. (2021). "An Investigation of tensile and thermal properties of epoxy polymer modified by activated carbon particle," *IOP Conference Series: Materials Science and Engineering* 1094(1), Article ID 012164. DOI: 10.1088/1757-899x/1094/1/012164
- Karak, N. (2021). "Overview of epoxies and their thermosets," *ACS Symposium Series* 1385, 1–36. DOI: 10.1021/bk-2021-1385.ch001
- Kubasad, P. R., Gawande, V. A., Todeti, S. R., Kamat, Y. D., and Vamshi, N. (2020). "Design and analysis of a passive ankle foot orthosis by using transient structural method," *Journal of Physics: Conference Series*, 1706(1). DOI: 10.1088/1742-6596/1706/1/012203
- Lee, S. M., Lee, S. H., and Roh, J. S. (2021). "Analysis of activation process of carbon black based on structural parameters obtained by XRD analysis," *Crystals* 11(2), Article Number 153. DOI: 10.3390/cryst11020153
- Mavroidis, C., Ranky, R. G., Sivak, M. L., Prittiti, B. L., DiPisa, J., Caddle, A., Gilhooly, K., Govoni, L., Sivak, S., Lancia, M., *et al.* (2011). "Patient specific ankle-foot orthoses using rapid prototyping," *Journal of NeuroEngineering and Rehabilitation* 8(1), Article Number 1. DOI: 10.1186/1743-0003-8-1
- Mohmad, M., Fadzli, M., Abdollah, B., Khudhair, A. Q., Tamaldin, N., Amiruddin, H., Bin, M. R., and Zin, M. (2018). "Physical mechanical properties of palm kernel activated carbon reinforced polymeric composite: Potential as a self lubricating material," *Jurnal Tribologi* 17(1), 77–92.
- Orthosis, A. (2006). *Manufacturing Guidelines for Ankle-Foot Orthosis*. Available online: <https://www.icrc.org/eng/assets/files/other/eng-afo-2010.pdf>
- Punyamurthy, R., Sampathkumar, D., Bennehalli, B., Patel, R., and Venkateshappa, S. C. (2014). "Abaca fiber reinforced epoxy composites: Evaluation of impact strength," *International Journal of Sciences: Basic and Applied Research* 18(2), 305–317.
- Raj, R., Dixit, A. R., Łukaszewski, K., Wichniarek, R., Rybarczyk, J., Kuczko, W., and Górski, F. (2022). "Numerical and experimental mechanical analysis of additively manufactured ankle-foot orthoses," *Materials* 15(17), Article Number 6130. DOI: 10.3390/ma15176130
- Salleh, Z., Yusop, M. Y. M., and Rosdi, M. S. (2013). "Mechanical properties of activated carbon (ac) coir fibers reinforced with epoxy resin," *Journal of Mechanical Engineering and Sciences* 5, 631–638. DOI: 10.15282/jmes.5.2013.9.0060
- Shahar, F. S., Hameed Sultan, M. T., Lee, S. H., Jawaid, M., Md Shah, A. U., Safri, S. N. A., and Sivasankaran, P. N. (2019). "A review on the orthotics and prosthetics and the potential of kenaf composites as alternative materials for ankle-foot orthosis," *Journal of the Mechanical Behavior of Biomedical Materials* 99, 169–185. DOI: 10.1016/j.jmbbm.2019.07.020
- Shakir, W.A., Mohammed, M.R., and Hilal, I. H. (2019). "Mechanical characteristics of (TiO₂-ZnO)/PMMA nanocomposites for dentures," *International Journal Medicine Research Health Sciences* 8 59-72.
- Singhal, P., Raghavan, S., Rattan, S., and Diwan, R. K. (2017). "Polypropylene/glass fiber composites for low cost orthotic aid," *Springer Proceedings in Physics* 178, 415-424. DOI: 10.1007/978-3-319-29096-6_54

- Sinha, A. K., Narang, H. K., and Bhattacharya, S. (2018). "Tensile strength of abaca epoxy laminated composites," *Materials Today: Proceedings* 5(14), 27861-27864. DOI: 10.1016/j.matpr.2018.10.024
- Sosiati, H., Anugrah, R., Binangun, Y. A., Rahmatullah, A., and Budiyanoro, C. (2019). "Characterization of tensile properties of alkali-treated kenaf/polypropylene composites," *AIP Conference Proceedings* 2097(1), Article ID 030113. DOI: 10.1063/1.5098288
- Sosiati, H., Firmansyah, F., & Rahman, M. B. N. (2022). "The role of silica in improving the properties of kenaf/silica/epoxy hybrid composites," *AIP Conference Proceedings* 2499(November). DOI: 10.1063/5.0104978
- Sosiati, H., Guntur Ma'arif, M., Firmansyah, W. A., and Hamdan, S. (2023). "Characterization of the properties of bio-CaCO₃ waste eggshell and abaca fiber reinforced hybrid composites," *Materials Science Forum* 1087, 13–20. DOI: 10.4028/p-n61z06
- Sosiati, H., Rizky, A. M., Latief, A. L. M., Adi, R. K., and Hamdan, S. (2023). "The mechanical and physical properties of microcrystalline cellulose (MCC)/sisal/PMMA hybrid composites for dental applications," *Materials Research Express* 10(3). DOI: 10.1088/2053-1591/acbb57
- Takhakh, A. M., and Abbas, S. M. (2018). "Manufacturing and analysis of carbon fiber knee ankle foot orthosis," *International Journal of Engineering and Technology(UAE)* 7(4), 2236-2240. DOI: 10.14419/ijet.v7i4.17315
- Walbran, M., Turner, K., and McDaid, A. J. (2016). "Customized 3D printed ankle-foot orthosis with adaptable carbon fibre composite spring joint," *Cogent Engineering* 3(1), Article ID 1227022. DOI: 10.1080/23311916.2016.1227022

Article submitted: August 3, 2023; Peer review completed: September 2, 2023; Revisions received: September 12, 2023; Revisions accepted: September 14, 2023; Published: September 18, 2023.

DOI: 10.15376/biores.18.4.7510-7523